10.1098/rsta.2002.1163

THE ROYAL SOCIETY

Dynamics of weakly aggregated colloidal particles

By Maria L. Kilfoil[1], Eugene E. Pashkovski[2], James A. Masters[2] and D. A. Weitz[1]

[1]*Department of Physics and DEAS, Harvard University, Cambridge, MA 02138, USA*
[2]*Colgate–Palmolive Co., 909 River Rd, PO Box 1343, Piscataway, NJ 08855-1343, USA*

Published online 4 March 2003

We discuss the behaviour of the dynamics of colloidal particles with a weak attractive interparticle interaction that is induced through the addition of polymer to the solvent. We briefly review the description of their behaviour in terms of the jamming phase diagram, which parametrized the fluid-to-solid transition due to changes in volume fraction, attractive energy or applied stress. We focus on a discussion of ageing of the solid gels formed by these colloid–polymer mixtures. They exhibit a delayed collapse induced by gravity. The time evolution of the height of the sediment exhibits an unexpected scaling behaviour, suggesting a universal nature to this delayed collapse. We complement these measurements of the scaling of the collapse with microscopic investigations of the evolution of the structure of the network using confocal microscopy. These results provide new insight into the origin of this ageing behaviour.

Keywords: colloidal aggregates; pastes; ageing; delayed sedimentation

1. Introduction

Colloids are ubiquitous in industry. They have a wide variety of uses: from paints to tyres, and from coatings to adhesives. They are used to control flow, optical characteristics, texture, stability and other physical properties. Their rheological behaviour can vary from a low-viscosity fluid to a highly elastic paste and can be controlled by the volume fraction of particles, ϕ, or the interaction between the particles. A polymer is often added to the solvent to further adjust the rheological properties; the polymer modifies the viscosity of the solvent, but can also induce an attraction between the particles due to depletion of the polymer (Asakura & Oosawa 1958; Vrij 1976; Mao *et al*. 1995). This attractive interaction can cause the particles to gel, forming a solid network at low volume fractions (Poon *et al*. 1995; Verhaegh *et al*. 1997; Dinsmore & Weitz 2002; Prasad *et al*. 2003).

The nature of the gelation can vary significantly as the properties of the colloidal suspension are varied. In an attempt to unify the disparate behaviour, the concept of a jamming phase transition was used to describe this fluid-to-solid transition (Trappe & Weitz 2000). The jamming phase diagram was first proposed by Liu

One contribution of 14 to a Discussion Meeting ‘Slow dynamics in soft matter’.

& Nagel (1998) to describe the behaviour of systems of repulsive particles. They suggest that the system can be made to undergo a fluid-to-solid transition or jam when the density, ρ, is increased, the temperature, T, is decreased or when some externally applied stress, σ, is decreased. Each of these three control parameters forms an axis on a three-dimensional phase diagram; they use ρ^1, T and σ as the axes so that the jammed state is the inner octant of the phase diagram, and a surface on this phase diagram represents the boundary between the jammed and fluidized states. A key insight that is inherent in this picture is the recognition that each of these quantities plays the same role in causing the system to jam; they each behave as an effective temperature. Liu & Nagel (1998) also recognized that the repulsive interactions between the particles require an additional stress to confine the particles. This can be an osmotic stress or some form of applied uniform stress. They also speculated that this external force could be replaced by a uniform attractive interaction between particles. This allows the jamming phase diagram to be applied to attractive colloidal systems (Trappe *et al*. 2001).

In the application of the jamming phase diagram to attractive colloidal particles the axes must be modified. The particle volume fraction plays the role of density and is set by the experiment; it does not vary with temperature in the same way as it can for repulsive particles. The temperature must be normalized by the strength of the attractive energy of interaction between particles, U; this gives U the same role as temperature in determining the phase behaviour. Thus, the three axes of the jamming phase diagram for attractive particles become ϕ^1, $k_{\mathrm{B}}T/U$ and σ. The jammed or solid state is again in the inner octant of this phase diagram. Crossing the phase boundary in any direction will cause a jammed state to be fluidized. This jamming phase diagram provides a good description of the behaviour of attractive colloidal particles (Trappe *et al*. 2001).

Some important supporting evidence for the jamming concept comes from the behaviour of a model system (Pusey & van Megen 1986) comprised of polymethylmethacrylate (PMMA) spheres, stabilized by thin layers of poly-12-hydroxystearic acid, suspended in a mixture of cycloheptylbromide (CHB) and decalin that matches both the index of refraction and the density of the particles (Prasad *et al*. 2003). An attractive depletion interaction is induced through the addition of polystyrene to the suspension (Pusey *et al*. 1993). The depth and range of the attractive depletion interaction between the colloidal particles is varied by changing the concentration of the polymer and the size of the polymer relative to the colloidal particles, respectively.

The onset of kinetic arrest of the system, and hence the jamming transition, can be measured in several ways. Dynamic light-scattering measurements made at scattering wave vectors sensitive to cluster motion can determine the phase boundary. These data show an ergodic-to-non-ergodic transition at a characteristic volume fraction, ϕ_{c}, and at a characteristic interaction energy, U_{c} (Segre *et al*. 2001; Prasad *et al*. 2003). In addition, the phase behaviour can be measured directly by rheology. The frequency-dependent elastic modulus $G'(\omega)$ and loss modulus $G''(\omega)$, determined by oscillatory measurements in the linear viscoelastic regime, can be scaled onto a single master curve as both U and ϕ are varied, provided the data are from samples in the solid regime (Trappe & Weitz 2000; Prasad *et al*. 2003). This allows the plateau elastic modulus to be determined even for very weak samples. For relatively large values of U, the elastic modulus exhibits a critical onset; for smaller values of U the onset is more similar to that of a glass, with the critical point determined by when

the slowest relaxation vanishes or goes to a frequency that is too low to be measured (Prasad *et al*. 2003). In all cases, however, we can identify the onset of the solid-like state.

In addition to the dependence on volume fraction and interaction energy, the gels also have a yield stress, the stress required to make the sample yield and flow, and hence become a fluid again. This yield stress can be determined as a function of both ϕ and U, and it forms the boundary on the third axis of the phase diagram, that of σ. This makes it possible to determine the three-dimensional jamming phase diagram for the system.

This is an appealing description of colloidal aggregation and gelation: while the detailed shape of the phase boundary depends on the details of the system, the overall behaviour is the same. However, there are many important features about the fluid-to-solid transition in attractive colloidal particles that are not described by this basic picture of jamming. The properties of the solid state can be quite dependent on the history of the sample; applying a small oscillatory strain to the sample while the gel is forming can dramatically modify the modulus of the solid (V. Trappe 1999, personal communication). Similarly, ageing can lead to large changes in the modulus as time evolves. These ageing effects can also dramatically alter the properties of the material and can lead to completely different behaviour.

One of these features, which does not directly modify the overall behaviour in these attractive jamming systems, is delayed sedimentation, or transient gelation, a non-equilibrium phenomenon that occurs in a variety of physical systems yet remains poorly understood (Pusey *et al*. 1993; Poon *et al*. 1999; Starrs *et al*. 2002). Its signature in colloidal systems is a sudden collapse of a system of colloidal particles, provided that their density differs from that of the solid. An intriguing feature of this behaviour is the delay; the particles initially form a stress-bearing network that is stable under gravity for an extended time, and then it rather suddenly collapses. This is one form of ageing of the sample.

In this paper, we focus on the sedimentation of a suspension of colloidal particles in a solvent that contains a polymer that modifies the viscosity of the solvent and induces an attractive interaction between the particles. We measure the height of the sample as it sediments, and show that the time evolution exhibits a surprising scaling behaviour. We use confocal microscopy on similar samples to obtain additional physical insight into the origin of the ageing and the delayed sedimentation of these samples.

2. Effect of ageing

To investigate the effects of ageing, we measure the time evolution of gels formed by colloid–polymer mixtures which have a density mismatch between the colloidal particles and the suspending fluid. We use 0.5 μm diameter silica spheres in carboxymethylcellulose (CMC), a biopolymer, which has a molecular weight of 40 000. The silica particles are negatively buoyant in the suspending fluid so that the particles sediment to the bottom of the sample cell. By measuring the frequency-dependent elastic modulus, $G'(\omega)$, and viscous modulus, $G''(\omega)$, of the polymer solutions, we determine that they are predominantly viscous liquids in the range of concentrations used here. The solvent is a mixture of water and glycerol, chosen to adjust the viscosity.

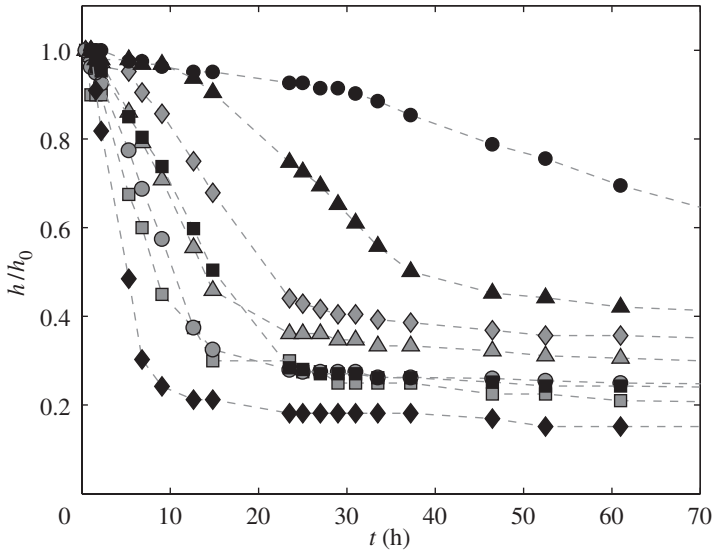

Figure 1. Sedimentation profiles for 0.5 μm silica/CMC/glycerol/water colloid–polymer mixtures at $\phi = 0.11$: black diamond, $C_p = 0.087$ wt%; black square, $C_p = 0.16$ wt%; black circle, $C_p = 0.25$ wt%; grey square, $C_p = 0.33$ wt%; grey triangle, $C_p = 0.5$ wt%; grey diamond, $C_p = 0.75$ wt%; black triangle, $C_p = 1.0$ wt%; black circle, $C_p = 1.5$ wt%. To account for slightly different initial heights, the height, $h(t)$, has been normalized by the initial height, h_0, for each profile. The profiles show the characteristic delay before collapse of the colloidal network.

We report on colloid–polymer mixtures in which ageing leads to destabilization and collapse of the particles under gravitational stress. All of the samples are prepared in glass vials at varying particle volume fraction and polymer concentration. We mix the samples prior to starting to measure them, ensuring that the particles are well dispersed. In samples which sediment, we observe the development of a smooth interface between a particle-rich sediment and the supernatant, which appears free of particles. We measure the height h of the particle-rich phase as a function of time. We define $t = 0$ as the time the sample is mixed and poured into its sample vial. Sedimentation profiles for one series of samples at a fixed volume fraction of $\phi = 0.11$ and varying polymer concentrations are shown in figure 1, where we plot the height, $h(t)$, as a function of the time, t. The profiles are characterized by slow or non-existent settling for a finite waiting time, followed by a sudden, catastrophic collapse of the colloidal particles. We measure the slope of the sedimentation profiles in the fastest part of the collapse and find that it is constant for a given sample. This indicates that the boundary between the colloidal particles and the supernatant moves at a constant rate during the fastest part of the collapse, so that the sedimentation proceeds at a constant velocity. The velocity itself is sample dependent. In the final stage, the sedimentation profiles level off as the height of the colloid-rich phase approaches a final height, at which it is again stable, under gravitational stress. The final height of the colloid-rich phase is unique to each polymer concentration. This collapse is exhibited by all of the samples which phase separate on time-scales we observe. The time-scale for the onset of the collapse becomes dramatically longer with increasing polymer concentration.

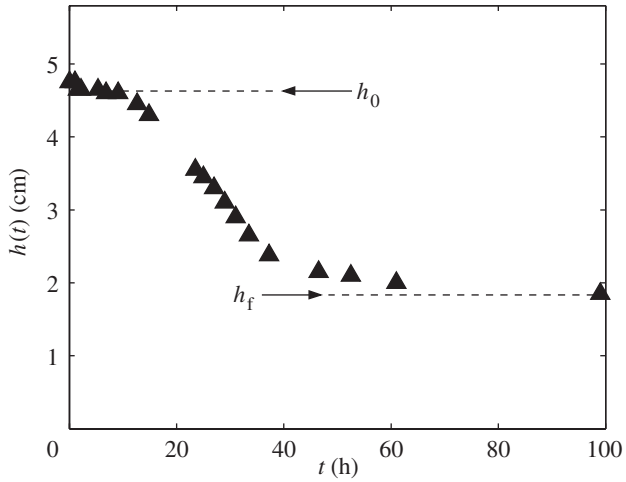

Figure 2. Schematic of the method used for normalization of sedimentation profiles prior to scaling: initial height of the colloid–polymer mixture, h_0, and the final height of the colloidal particles, h_f. In the fastest part of the sedimentation profile the slope is constant and yields the sedimentation velocity during the collapse.

To compare the profiles, the height is first normalized to the initial height, $h_0 = h(t = 0)$, of the sample, shown for a typical sample in figure 2. All of the samples were prepared at approximately the same initial height. To account for the different final sediment heights at different polymer concentrations, all of the profile height data for each sample are also normalized to the final height of the colloid-rich phase, $h_f = h(t \gg \tau)$, as shown in figure 2; thus, we plot as a function of time the relative collapse of the particle-rich phase, $h'(t) = (h(t)-h_f)/(h(t)-h_f)(h_0-h_f)(h_0-h_f)$, for each polymer concentration. On eliminating the difference in final volume fraction, all of the sedimentation profiles have the same characteristic form. They all exhibit a plateau at $h'(t) = 1$ at short times and the crossover to $h'(t)$ approaching zero at long times. They differ in the time-scale at which they turn over.

Remarkably, the normalized sedimentation profiles can all be scaled together onto a single master curve. We do this by scaling the time; a typical example of a master curve, for $\phi = 0.11$, is shown in figure 3. Similar scaling behaviour is seen for other volume fractions, and data for each ϕ can be scaled onto a master curve for that dataset. The shape of the master curve varies somewhat for the different volume fractions, but the scaling behaviour remains robust.

The behaviour we observe in these samples is reminiscent of the delayed sedimentation observed in PMMA gels (Pusey *et al*. 1993; Poon *et al*. 1999; Starrs *et al*. 2002). In both systems the polymer induces an attractive interaction between the particles and there is a density mismatch between the particles and the suspending fluid. Furthermore, a structure is formed which is stable for some finite time after which catastrophic collapse and sedimentation occurs. Delayed sedimentation has also been observed in other colloid–polymer systems (Verhaegh *et al*. 1997, 1999) and in depletion-flocculated oil-in-water emulsions (Parker *et al*. 1995; Manoj *et al*. 1998). The shape of the unscaled sedimentation profiles in figure 1 is similar to that observed previously in PMMA transient gels. However, this scaling behaviour has not been reported previously.

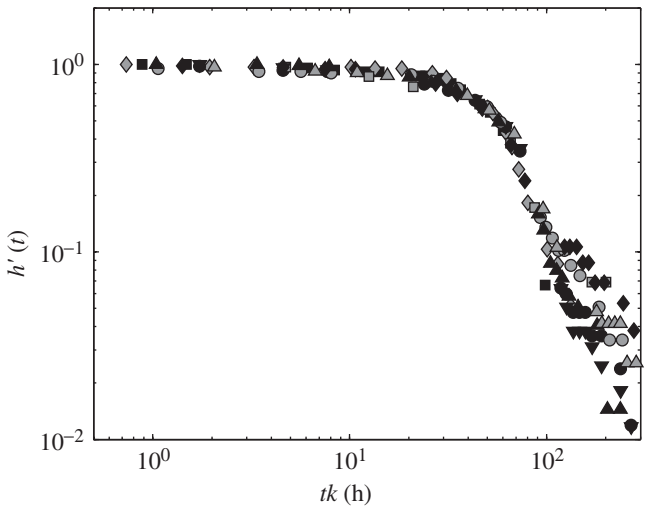

Figure 3. Master curve showing the normalized profiles as a function of scaled time for all data in figure 1, at $\phi = 0.11$ and varying polymer concentration C_p. The scale factors yield the delay time τ for the onset of the collapse for each polymer concentration.

The data for different polymer concentrations for each volume fraction of colloid are all scaled onto the set that has the longest delay time; from this, we determine the factor, k, required to scale the times. We define the delay time τ_M for the collapse for the sample with the longest delay to be $h'(\tau_\mathrm{M}) = 0.1$. From the scale factor k, we determine the absolute delay time for each sample of a series of samples at fixed ϕ: $\tau(C_\mathrm{p}) = \tau_\mathrm{M}/k$. By scaling together the sedimentation data at different ϕ we obtain the delay $\tau(\phi, C_\mathrm{p})$ as a function of the particle volume fraction and polymer concentration of the system.

The scaling suggests that the wide variation in time-scale for the onset of delayed sedimentation observed for these weakly attractive colloid–polymer mixtures can be significantly simplified. The system shows the same approach to instability and the same dynamic behaviour during the phase separation, independent of the details of the preparation of the system.

The dependence of the delay time, τ, on polymer concentration for $\phi = 0.11$ is shown by the solid points in figure 4. The delay time is obtained from the scaling of the sedimentation data for a single particle volume fraction onto the master curve for that volume fraction. The sedimentation profiles were also studied for $\phi = 0.055$, $\phi = 0.15$, $\phi = 0.175$ and $\phi = 0.20$ at varying polymer concentrations. For each ϕ, the same sedimentation phenomenon was observed and the data for different polymer concentrations could again be scaled together onto a single curve and the delay times could thus be obtained. The C_p-dependence of the delay time for the lowest volume fraction, $\phi = 0.055$, is nearly identical to that for $\phi = 0.11$, as shown by the open symbols in figure 4.

The delay times for all C_p and ϕ that we measured are plotted together in figure 5*a*. We find that τ determined from the scaling of the sedimentation data for a single ϕ depends exponentially on polymer concentration, $\tau \sim \tau_0 \exp(\beta C_\mathrm{p})$. The dependence, characterized by β, is different for each volume fraction. We plot $\beta(\phi)$ as a function of ϕ in figure 5*b*; $\beta(\phi)$ is nearly independent of ϕ at lower volume

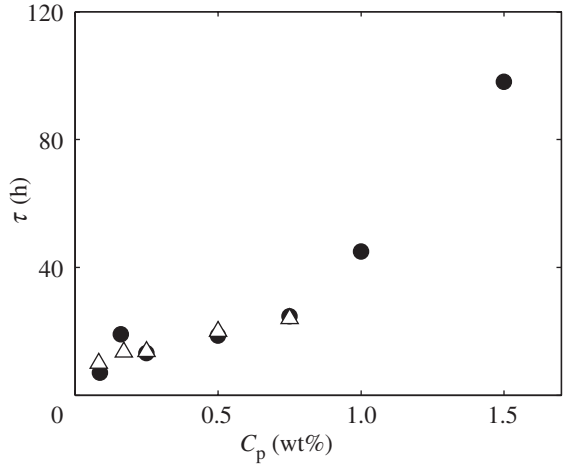

Figure 4. Dependence of onset time for the delayed collapse on C_p for $\phi = 0.11$ (solid symbols) and $\phi = 0.055$ (open symbols).

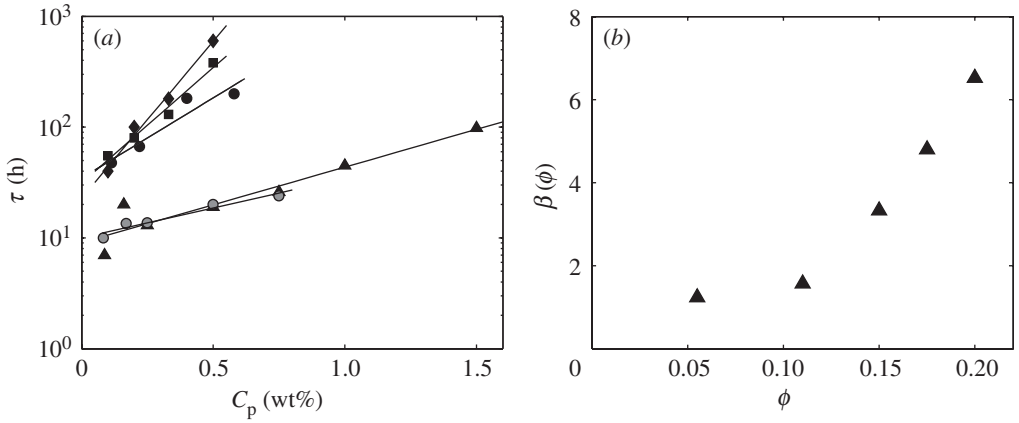

Figure 5. (*a*) Dependence of the delay time, τ, determined from the scaling, on polymer concentration for different ϕ; when the delay times are plotted logarithmically in time as a function of C_p, all of the data for each ϕ fall onto a straight line. Grey circle, $\phi = 0.055$; black triangle, $\phi = 0.11$; black circle, $\phi = 0.15$; black square, $\phi = 0.175$; black diamond, $\phi = 0.20$. (*b*) Exponential dependence, β, plotted as a function of ϕ; $\beta(\phi)$ is nearly independent of ϕ for $\phi \leqslant 0.10$, and it increases roughly linearly with ϕ for $\phi > 0.10$.

fractions, $\phi \leqslant 0.10$, and it increases roughly linearly with ϕ at higher volume fractions, $\phi > 0.10$. Hence for $\phi > 0.10$ the time-scale also increases exponentially with ϕ. All of the samples for the silica–CMC system follow this same phenomenological behaviour.

The dependence of the time-scale on the polymer concentration gives insight into the effect of the interaction energy. The polymer, presumably, induces a depletion attraction; increasing the concentration of the polymer increases the strength of the interparticle attraction. These stronger interparticle interactions slow the dynamics of the evolution of the system.

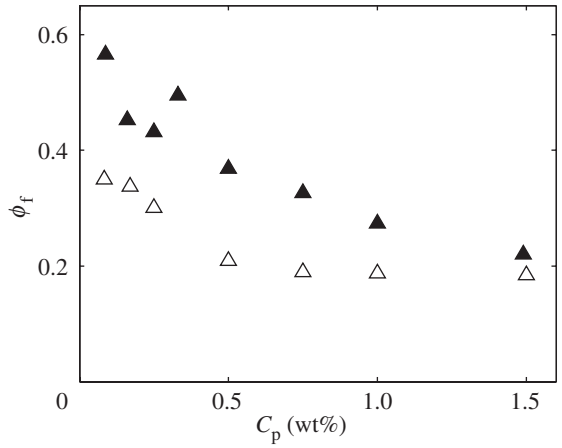

Figure 6. Comparison of final colloid volume fraction, ϕ_f, of the collapsed state for starting volume fractions, $\phi = 0.11$ (solid symbols) and $\phi = 0.055$ (open symbols). ϕ_f decreases as C_p is increased. The final state is more collapsed for starting volume fraction $\phi_i = 0.11$ than for $\phi_i = 0.055$, with ϕ_f approaching 0.20 at high polymer concentration in both cases.

As further evidence that interparticle interaction energy increases with polymer concentration, the sedimentation profiles at fixed volume fraction and varying polymer concentrations reach different asymptotic values at large times. The final volume fraction ϕ_f is obtained from the initial and final heights and the known initial volume fraction. For $\phi = 0.11$, the final sediment is less densely packed for higher polymer concentrations, as shown by the solid symbols in figure 6. The colloidal particles settle until their volume fraction is such that their dynamics again become arrested and they can again support a load. The decrease in ϕ_f with increasing C_p is consistent with a stronger interaction between the particles, which leads to more tenuous structures. As the initial volume fraction decreases, the final volume fraction also decreases, as shown by the open symbols in figure 6. Interestingly, however, all volume fractions seem to approach the same value of $\phi_f = 0.20$, independent of the starting volume fraction. This suggests that samples at starting volume fractions exceeding $\phi = 0.20$ and polymer concentrations above 1 wt% would never become unstable as they are already above this metastable criterion. Consistent with this, we have observed that samples meeting this have not become unstable after five months.

When the collapse begins, we find that the slope of the sedimentation profile is approximately linear, implying that the collapse proceeds with a constant velocity. In this region we measure the velocity, $v = \mathrm{d}h(t)/\mathrm{d}t$, and plot its dependence on polymer concentration in figure 7*a* for $\phi = 0.11$; the velocity decreases with polymer concentration. Because the viscosity sets the scale for the dynamics, we also determine the zero-shear dynamic viscosity η_0 of the suspending fluid, obtained by measuring the steady shear viscosity $\eta(\dot{\gamma})$ over a range of shear rates and taking as η_0 the viscosity in the low-shear plateau; the dependence on C_p is plotted in the inset of figure 7*a*. The increase in viscosity with polymer concentration will contribute to the decrease in sedimentation velocity. To remove the effect of the viscosity, we plot the velocity normalized by η_0 in figure 7*b*. Despite the decrease in absolute velocity with polymer concentration, when velocity is normalized by the viscosity of the background fluid, it *increases* with the polymer concentration; this must reflect the

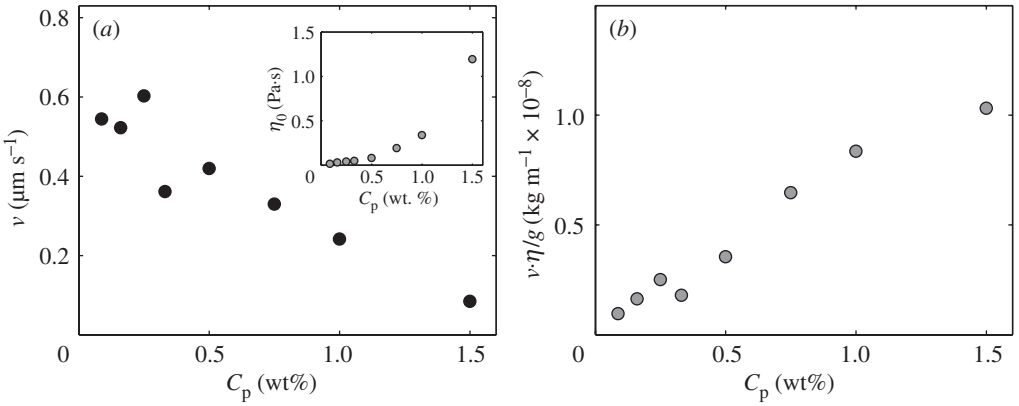

Figure 7. Sedimentation velocity, v, of the gel as a function of C_p for $\phi = 0.11$. (*a*) v calculated from the raw sedimentation-height data in the fastest part of the collapse where v is constant for each profile. Inset shows the zero shear viscosity of the suspending fluid plotted versus polymer concentration. (*b*) v normalized by the viscosity, η_0, versus C_p.

effect of interparticle attractions induced by the polymer. One possibility is that the attractive interaction changes the nature of the structure, and clusters grow larger and settle more rapidly with a stronger interaction between the particles.

The system studied here is closely related to the PMMA system, suggesting that the behaviour we observe is similar to the transient gelation observed in PMMA (Pusey *et al*. 1993; Poon *et al*. 1999; Starrs *et al*. 2002). However, we do not observe the large-scale structures seen in the gravitational collapse of the transient PMMA gels (Starrs *et al*. 2002), where dark-field microscopy reveals channels and streamers that seem to involve transport of colloids upward during the early stages of the delay and expulsion of the solvent from the colloid-rich phase during the late stages of the delay.

The picture that emerges from the sedimentation data is that the colloidal particles initially exist as a homogeneous mixture of monomers when they are first mixed, and then aggregate into a sample-spanning colloidal network which is elastic and supports the weight of the particles. Following a delay time, the system evolves to a state of incipient failure and suddenly collapses catastrophically under its own weight. Ageing of the colloid–polymer mixtures leads to evolution of mechanical stability. This suggests that there is some evolution taking place in the microstructure during this ageing process. While the scaling behaviour we observe greatly simplifies the wide variation in time-scale for the delayed collapse of a network in colloid–polymer mixtures, it does not provide any insight into what is structurally causing the delayed sedimentation.

To investigate the structure directly, we use confocal microscopy to study colloid–polymer mixtures; for this, we use 1 μm diameter, fluorescently labelled colloidal polystyrene latex particles in CMC dispersed in a water and glycerol mixture. In the polystyrene–CMC mixtures the particles are positively buoyant, and thus they rise to the top of the sample cell after the delay time. The samples are prepared for confocal microscopy in a sealed, square well, *ca.* 10 mm on each side and 200 μm deep. The glycerol–water suspending fluid is maintained at 90% glycerol ($n = 1.47$), 10% water ($n = 1.33$) for the confocal microscopy studies to match as closely as

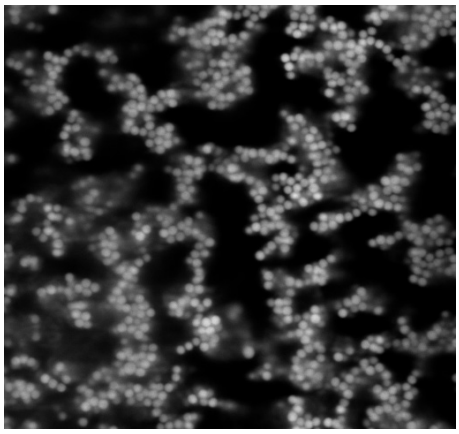

Figure 8. Slice of a gel of colloidal particles seen in confocal microscopy. The micrograph represents a 44 μm × 40 μm region at a depth of 6 μm into the sample away from the cover slip.

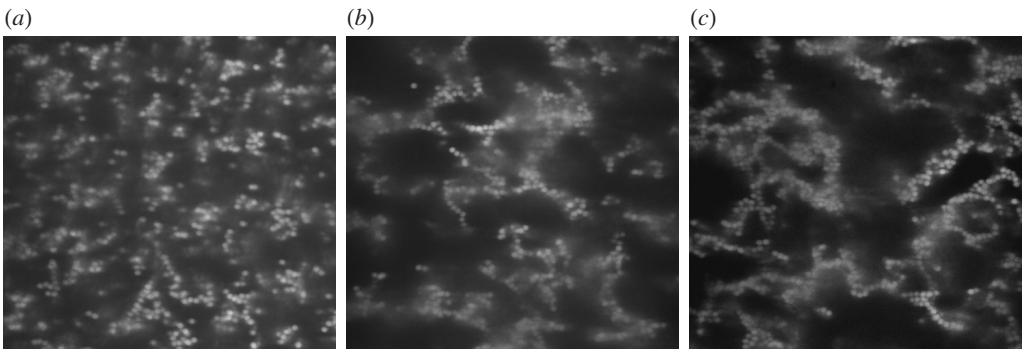

Figure 9. Structural evolution and coarsening during ageing of colloid–polymer mixtures. (*a*) 2 h, colloidal particles exist as monomers. (*b*) 1 day, colloidal network with only very few monomers remaining. (*c*) 4 days, the colloidal gel has aged, showing evidence of coarsening.

possible the refractive index of the latex particles ($n = 1.59$). However, because the true index-matching condition cannot be met, some light is scattered by the particles. This limits the depth to which we are able to image the sample; nevertheless, we are still able to acquire images of the structure to greater than 20 μm into the sample. We can thus carry out true three-dimensional imaging of the sample well away from the surface.

The micrographs provide qualitative support that the particles form a space-spanning, interconnected network, shown by a cross-sectional image of a typical sample in figure 8. The gel forms from the dispersed colloids, with very few monomers remaining in the suspension. The network is connected by chains of particles which are typically quite tenuous in the early stages of the gel. There appears to be a characteristic length-scale to the gel, which presumably corresponds to the spacing between the clusters that comprise the network, and is about eight particle diameters, or 8 μm. Whether the structure comprises a truly space-spanning gel was not ascertained from the microscopy. The network fluctuates due to thermally induced fluctuations, as expected for a weak solid.

We also occasionally observe instances of the sudden collapse directly with confocal microscopy. We observe a colloidal gel which has aged and is fixed in space and undergoing thermal fluctuations; suddenly it disappears from the focal plane in the direction against the Earth's gravitational field. The colloidal particles collapse either as a single network or as individual locally dense clusters; however, the mechanism driving the collapse remains unclear. In addition, we image the structure during the induction period preceding the catastrophic failure. While there are no observable large-scale structural rearrangements during the induction period, there are small structural rearrangements of chains of particles leading to reorganization of the connectivity on the length-scale of a few particle diameters; however, these rearrangement events are rare. The series of micrographs in figure 9 provides a qualitative picture of the consequences of the rearrangements; this sequence of images is typical of the structural evolution we observe. From the homogeneous mixture of colloid monomers pictured in part (*a*), the colloids form the tenuous network of colloids pictured in part (*b*). With ageing of the sample, we observe some degree of slow coarsening of the microstructure with time, with the particles packing more densely in some localized regions. The microscopy suggests that the length-scale of the local structure evolves as the colloidal gel ages.

3. Conclusion

Systems of colloid–polymer mixtures exhibit a delayed sedimentation with an unexpected scaling behaviour. When the system is first mixed, it is quenched and the particles exist initially as a homogeneous, random mixture of colloidal particles. The colloids then form a disordered condensed phase: a space-spanning gel. The system becomes trapped in a non-equilibrium state, with arrested or very slow internal dynamics and a metastable morphology. It then undergoes slow restructuring in such a way that the morphology of the colloidal network changes, some structural integrity is lost, and the (constant) weight of the particles under gravity causes collapse. The delay time that we observe is the onset time for instability under gravity, and signals the collapse of the network. The sedimentation profiles for samples with different volume fractions scale together onto a master curve. Similar master curves are found for different volume fractions; their shapes differ slightly, but the scaling behaviour remains robust.

We expect this scaling behaviour to be quite general for kinetically arrested systems. The same behaviour is observed for the PMMA depletion gels. This scaling should help provide useful predictive capabilities for these sorts of gels, which may find considerable value in predicting the stability of technical colloid systems.

We thank Veronique Trappe, Wilson Poon and Alan Parker for helpful discussions. We also gratefully acknowledge support from Colgate–Palmolive, the NSF through the Harvard Materials Research Science and Engineering Center (DMR-0213805), and the NSERC (M.L.K.).

References

Asakura, S. & Oosawa, F. 1958 Interaction between particles suspended in solutions of macromolecules. *J. Polymer Sci.* **33**, 183–192.

Dinsmore, A. D. & Weitz, D. A. 2002 Direct imaging of three-dimensional structure and topology of colloidal gels. *J. Phys. Condens. Matter* **14**, 7581–7597.

Liu, A. J. & Nagel, S. R. 1998 Jamming is not just cool anymore. *Nature* **396**, 21–22.

Manoj, P., Fillery-Travis, A. J., Watson, A. D., Hibberd, D. J. & Robins, M. M. 1998 Characterization of a depletion-flocculated polydisperse emulsion. *J. Colloid Interface Sci.* **207**, 283–293.

Mao, Y., Cates, M. E. & Lekkerkerker, H. N. W. 1995 Depletion force in colloidal systems. *Physica* A **222**, 10–24.

Parker, A., Gunning, P. A. & Robins, M. M. 1995 How does xanthan stabilise salad dressing. *Food Hydrocoll.* **9**, 333–342.

Poon, W. C. K., Pirie, A. D. & Pusey, P. N. 1995 Small angle light scattering investigation of phase separation and transient gelation in colloid–polymer mixtures. *Faraday Disc.* **101**, 65–96.

Poon, W. C. K., Starrs, L., Meeker, S. P., Moussaid, A., Evans, R. M. L., Pusey, P. N. & Robins, M. M. 1999 Delayed sedimentation of transient gels in colloid–polymer mixtures: dark-field observation, rheology and dynamic light scattering studies. *Faraday Disc.* **112**, 143–154.

Prasad, V., Trappe, V., Dinsmore, A. D., Segre, P. N., Cipaletti, L. & Weitz, D. A. 2003 Viscoelasticity of weakly aggregating depletion gels. *Faraday Disc.* **123**, 1–12.

Pusey, P. N. & van Megen, W. 1986 Phase-behavior of concentrated suspensions of nearly hard colloidal spheres. *Nature* **320**, 340–342.

Pusey, P. N., Pirie, A. D. & Poon, W. C. K. 1993 Dynamics of colloid polymer mixtures. *Physica* A **201**, 322–331.

Segre, P. N., Prasad, V., Schofield, A. B. & Weitz, D. A. 2001 Glass-like kinetic arrest at the colloid gelation transition. *Phys. Rev. Lett.* **86**, 6042–6045.

Starrs, L., Poon, W. C. K., Hibberd, D. J. & Robins, M. M. 2002 Collapse of transient gels in colloid–polymer mixtures. *J. Phys. Condens. Matter* **14**, 2485–2505.

Trappe, V. & Weitz, D. A. 2000 Scaling of the viscoelasticity of weakly attractive particles. *Phys. Rev. Lett.* **85**, 449–452.

Trappe, V., Prasad, V., Cipelletti, L., Segre, P. N. & Weitz, D. A. 2001 Jamming phase diagram for attractive particles. *Nature* **411**, 772–775.

Verhaegh, N. A. M., Asnaghi, D., Lekkerkerker, H. N. W., Giglio, M. & Cipaletti, L. 1997 Transient gelation by spinodal decomposition in colloid–polymer mixtures. *Physica* A **242**, 104–118.

Verhaegh, N. A. M., Asnaghi, D. & Lekkerkerker, H. N. W. 1999 Transient gels in colloid–polymer mixtures studied with fluorescence confocal laser microscopy. *Physica* A **264**, 64–74.

Vrij, A. 1976 Polymers at interfaces and the interactions in colloidal dispersions. *Pure Appl. Chem.* **48**, 471–483.

Discussion

P. Warren (*Unilever R&D Port Sunlight, Bebington, UK*). Coarsening in microgravity: spinodal decomposition shows a domain size growing approximately as $t^{2/3}$, as expected for inertial-regime spinodal decomposition. Is this the right interpretation? You would expect to see weakly damped oscillations in the interface (capillary waves). Can one estimate a Reynolds number?

D. A. Weitz. While one long-time behaviour of spinodal decomposition is predicted to be growth of the characteristic length-scale as approximately $t^{2/3}$, I do not believe that is the origin of the behaviour that we observe. The predicted behaviour arises from inertial effects, and I do not believe that inertia can play a role in this colloid system. Instead, I believe that there is some new physics that I do not, as yet, understand that leads to this behaviour, and that has to do with the separation of a

colloid-poor region from a colloid-rich region. We did look specifically for capillary waves at the interface, and we did not observe them. If we estimate the Reynolds number for the system, we can use the data to estimate

$$Re \approx \frac{l\dot{l}}{\nu} \approx \frac{l^2}{\nu t} \approx \frac{\pi^2}{q^2 \nu t} \approx \frac{10}{10^4 10^{-2} 10^4} \approx 10^{-5} \ll 1,$$

where I have used the average velocity, $\dot{l} \approx lt$, for the velocity, and where I take the characteristic length-scale to be $l \approx \pi q$, where q is the wave vector of the characteristic length-scale, and where I have approximated the viscosity as $\nu \approx 10^{-2}\ \mathrm{cm}^2\ \mathrm{s}^{-1}$. This is a very rough estimate, but it does show that the Reynolds number is much less than 1, so that inertial effects are unlikely to be important.

M. Nicodemi (*Department of Physical Sciences, University of Napoli, Italy*). Would you briefly discuss the relations between 'jamming', 'gelling' and 'critical slowing down'?

D. A. Weitz. Jamming is something that we use to refer to a fluid-to-solid transition because of kinetic arrest due to crowding of the constituent particles that ultimately comprise the solid material. Jamming therefore encompasses gelation; however, it is meant to be more broad than gelation, as it also encompasses fluid-to-solid transitions that are more commonly described as glass transitions. Our point is that gelation and the glass transition have many features in common, and we attempt to highlight this by calling it the jamming transition. Critical slowing down might refer to all the dynamics just prior to the jamming transition, since it is meant to reflect an arrest of the kinetics.

W. T. Coffey (*School of Engineering, Trinity College Dublin, Ireland*). The stretched or enhanced exponential behaviour you have mentioned is reminiscent of the behaviour suggested by the continuous-time random-walk model with a finite jump-length variance but a divergent characteristic waiting time, i.e. a long rests model. This would appear to lend support to your jamming hypothesis.

D. A. Weitz. While there is an analogy, it is not clear that there is anything that would have the physical properties of a continuous-time random walk.

B. U. Felderhof (*RWTU, Aachen, Germany*). You showed interesting data on the real and imaginary parts of the elastic shear modulus as a function of frequency. It would be useful to divide by frequency and plot instead the real and dynamic parts of the dynamic viscosity. These are related by Kramers–Kronig relations. Some years ago, Cichocki and I (Cichocki & Felderhof 1994) proposed a phenomenological description of the complex dynamic viscosity in terms of an expression suggested by an exact calculation for a semi-dilute hard-sphere suspension (Cichocki & Felderhof 1991). The dynamic viscosity is represented by a function with three poles in the square-root-of-frequency plane. Have you compared your data with analytic representations of this type?

D. A. Weitz. We have not compared our data with this representation. It would certainly be an interesting thing to try. However, it is important to point out that the rheological data we obtain presumably reflect a dominant contribution of the solid network. It would, therefore, be somewhat surprising if a model meant to describe

the behaviour of hard spheres were also able to describe the behaviour of a network of attractive particles.

R. C. Ball (*Department of Physics, University of Warwick, Coventry, UK*). To distinguish between irreversible aggregation and spinodal decomposition as paradigms for the observed gelation, consider looking at systems with a mixture of particle sizes.

Larger particles have larger depletion forces; this does influence selection in spinodal decomposition, but not in irreversible aggregation.

D. A. Weitz. An excellent idea.

Additional references

Cichocki, B. & Felderhof, B. U. 1991 Linear viscoelasticity of semi-dilute hard sphere suspension. *Phys. Rev.* A **43**, 5405–5412.

Cichocki, B. & Felderhof, B. U. 1994 Linear viscosity of dense colloidal suspensions. *J. Chem. Phys.* **101**, 7850–7855.